

## Observation of a BCS Spectral Function in a Conventional Superconductor by Photoelectron Spectroscopy

F. Reinert,\* G. Nicolay, B. Eltner, D. Ehm, S. Schmidt, and S. Hüfner

*Universität des Saarlandes, Fachrichtung 7.2—Experimentalphysik, D-66041 Saarbrücken, Germany*

U. Probst and E. Bucher

*Universität Konstanz, Fakultät für Physik, D-78434 Konstanz, Germany*

(Received 27 April 2000)

We present high-resolution photoelectron spectra on the A15-type conventional superconductor  $V_3Si$ , where—for the first time—both singularities of the BCS density of states can be resolved by photoemission spectroscopy (PES). With a transition temperature of about  $T_c \approx 17$  K the gap  $\Delta_{\text{gap}}$  of this compound has a magnitude of approximately 5 meV. A measurement by PES on this small energy scale requires a very high energy resolution ( $\Delta E \lesssim 5$  meV) and sample temperatures significantly below  $T_c$ .

PACS numbers: 74.25.Jb, 71.30.+h, 74.70.Ad, 79.60.Bm

Since the discovery of high-temperature superconductors (HTSC) [1] the study of conventional, metallic superconducting alloys has been pushed into the background of scientific research. Whereas the mechanisms of superconductivity in HTSCs are highly complex and far from being completely understood, the theory that describes the properties of the conventional weak-coupling superconductors was already developed in the 1950s and is based on the work of Bardeen, Cooper, and Schrieffer (BCS) [2]. The key concept of this theory is the electron-phonon interaction which—below the transition temperature  $T_c$ —correlates two electrons to a Cooper pair. The result of this pairing is a lowering of the total energy of the system and the opening of a narrow gap of the order of a few meV in the electronic density of states (DOS) around the Fermi level.

Among the conventional superconducting systems especially the intermetallic compounds of the A15 family ( $\beta$  tungsten structure) [3] show relatively high transition temperatures up to  $T_c = 20$  K, which is of course low in comparison to the transition temperatures of the HTSCs. These systems have been widely studied by various experimental techniques, for example by neutron and electronic Raman scattering [4–6], de Haas-van Alphen effect [7], and especially tunneling spectroscopy [8–10], which is apart from photoemission spectroscopy the method of choice to investigate the electronic density of states directly.

Photoemission spectroscopy (PES)—where photoelectrons, excited by monochromatic radiation, are analyzed in respect to angular and kinetic energy distribution—has been successfully applied to the study of the normal state Fermi surface and the superconducting gap of HTSCs [11] with typical total gap widths of the order of  $\Delta_{\text{gap}} = 50$  MeV.

Until very recently, PES on solids has not been able to resolve structures on the energy scale of a few meV, required for the determination of a gap in the spectral function of a conventional superconductor. The first observa-

tion of an unusual temperature dependence of PE spectra at the Fermi energy, which deviates from the one of a normal metal, was published by M. Grioni *et al.* [12]. But due to the finite energy resolution of  $\Delta E = 13$  meV, which is large in comparison to the gap width  $\Delta_{\text{gap}}$  of the investigated system ( $Nb_3Al$ ,  $T_c = 18.6$  K), the observed effect was small and the analysis of the data yields only an estimate of the BCS parameters like gap width or transition temperature.

In this paper we present temperature dependent photoemission spectra on the A15 compound  $V_3Si$  with a high energy resolution of  $\Delta E \approx 2.9 \pm 0.2$  meV which allows us to resolve the spectral features characteristic for the BCS model. The bulk transition temperature of  $V_3Si$  is about  $T_c = 17.1$  K [3], but it is known that disorder [13] and surface effects [9] can lower the transition temperature by several kelvin. Half the superconducting gap energy at  $T = 0$  amounts to  $\varepsilon_0 = \frac{1}{2} \Delta_{\text{gap}} = 2.6 \pm 0.2$  meV [4–8]. To avoid an influence of the martensitic phase transition at  $T_m \approx 21$  K [3] to the spectra, we have performed all our experiments at temperatures below  $T \leq 20$  K.

The PE experiments have been performed with a SCIENTA SES200 spectrometer and a monochromatized GAMMADATA vacuum ultraviolet (VUV) lamp at  $h\nu = 21.23$  eV (He I). The base pressure of the UHV system amounts to  $5 \times 10^{-11}$  mbar. During the measurement the pressure increased to  $8 \times 10^{-10}$  mbar due to the helium leakage from the discharge cavity. The sample temperature could be changed from approximately 10 K to room temperature, with an accuracy of approximately 1 K. The energy resolution of the analyzer system was determined by measuring a Fermi edge of a cooled silver sample, giving a value of  $\Delta E = 2.9 \pm 0.2$  meV (cf. Ref. [14]).

The  $V_3Si$  crystals were grown by chemical vapor transport technique in the temperature range from 1000 to 1100 °C, using bromine as a transport agent in a small quartz ampoule sealed under vacuum. The product was checked by x-ray diffraction techniques. The size of the

polycrystalline and single-crystalline  $V_3Si$  samples for the PES experiments was typically about  $2 \times 2 \times 2 \text{ mm}^3$ . Prior to the measurement the surface was prepared by *in situ* fracturing the crystals at low temperatures  $T < 20 \text{ K}$ . This procedure resulted in comparatively uneven and rugged surfaces that—in the case of single crystals—did not show any angular dependence in the spectra. Because of this increased effective angular integration we see a uniform DOS close to the Fermi level, although the calculated band structure shows several bands in the investigated energy range [15]. The quality of the sample surfaces was checked by core-level photoemission x-ray photoemission spectroscopy (XPS) which showed no carbon or oxygen contaminations. However, some of the prepared surfaces did not show any BCS like photoemission spectra or showed a mixture of a BCS and a large fraction of a normal metallic DOS.

To compare the experimental data to theoretical calculations we refer to the original work of Bardeen, Cooper, and Schrieffer [2], wherein the electronic DOS of a weak superconductor is given as a function of energy and temperature.

Here, the ratio of the energy gap  $\varepsilon_0$  at  $T = 0 \text{ K}$  to the transition temperature  $T_c$  is predicted to be the same for all superconductors and can be given (in the weak-coupling limit [2]) by

$$2\varepsilon_0/k_B T_c = 3.5. \quad (1)$$

The temperature dependence of the gap at finite temperature below  $T_c$  is given by a universal function of  $T/T_c$ , defined by an integral equation which cannot be solved analytically. Close to  $T_c$  this universal function can be approximated by

$$\begin{aligned} \varepsilon(T) &= 3.2k_B T_c \sqrt{1 - \frac{T}{T_c}} \\ &= 1.81\varepsilon_0 \sqrt{1 - \frac{T}{T_c}}. \end{aligned} \quad (2)$$

At lower temperatures  $\varepsilon(T)$  increases more slowly and approaches  $\varepsilon_0$  below  $T \approx \frac{1}{2} T_c$  (cf. inset of Fig. 4).

The theoretical BCS density of states at finite temperatures  $T < T_c$  has a gap of  $2\varepsilon(T)$  centered about the Fermi energy and is given for  $|E| \geq \varepsilon(T)$  by

$$\frac{dN(E, T)}{dE} = N(0) \frac{|E|}{\sqrt{E^2 - \varepsilon(T)^2}}, \quad (3)$$

which is singular at the edges of the gap  $E = \pm\varepsilon(T)$ . Inside the gap the DOS is zero.  $N(0)$  is the DOS of the Bloch-states at  $E = E_F = 0$ . For temperatures above  $T_c$  the density of states is assumed to be constant in energy [given by  $N(0)$ ]. The angular integrated photoemission spectrum measures only the occupied DOS, therefore the BCS DOS given above has to be multiplied by the Fermi-Dirac distribution at the experimental sample temperature.

Figure 1 shows a sketch of the BCS DOS at three different temperatures below  $T_c$ . The left hand side of the energy axis corresponds to the energies below  $E_F$  where

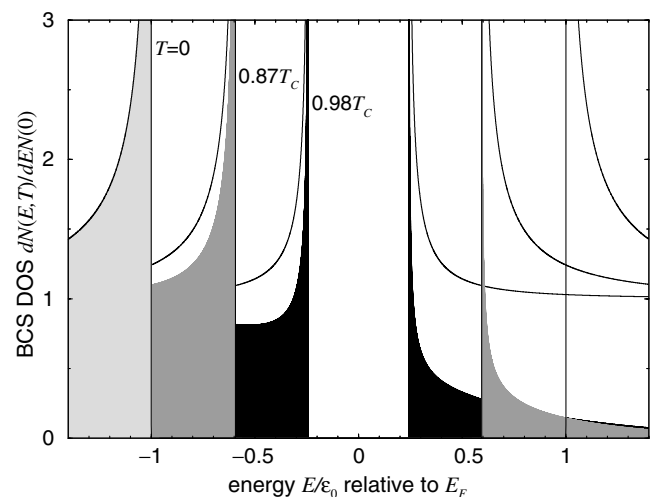


FIG. 1. Theoretically calculated density of states (DOS) from Ref. [2] for three different temperatures  $T < T_c$  (solid lines) with  $T_c = 17.1 \text{ K}$  (see text). The DOS shows a symmetric gap around the Fermi level  $E_F$  at  $E = 0$ , which decreases for temperatures approaching  $T_c$ . The filled areas describe the thermally occupied states at the respective temperature.

$N(E, T = 0)$  describes the occupied density of states. According to Eq. (3) each spectrum shows two square-root singularities at  $\pm\varepsilon(T)$  defining the gap. Increasing the temperature has two independent effects: (1) the states above  $E_F$  will be thermally occupied, described by the Fermi-Dirac statistics, and (2) both the gap widths and the enhanced DOS at the gap edges decrease, finally reaching a constant metallic DOS at temperatures  $T > T_c$  (not shown).

Experimentally, the finite energy resolution of the photoelectron spectrometer leads to a broadening of the DOS structures which can be described by a convolution with an appropriate spectrometer function. The spectrometer function is well approximated by a Gaussian, for which the full width at half maximum (FWHM)  $\Delta E$  gives the energy resolution of the system. This parameter can be extracted from the measurement of metallic Fermi edges at very low temperatures ( $4k_B T < \Delta E$ ) or from gas phase measurements. For our system we got a net energy resolution of  $\Delta E = 2.9 \pm 0.2 \text{ meV}$ . No further broadening was applied to the BCS DOS to describe the experimental data. The position of the energy zero is taken from the reference spectra of the Ag Fermi edge, but due to the steepness of the  $V_3Si$  spectra a fine tuning of  $\approx \pm 0.2 \text{ meV}$  was allowed in the least-squares analysis of the data.

To describe the (possible) fraction of the surface with normal metallic properties we add a constant density of states  $C = \text{const}$ , which is cut off by the Fermi-Dirac distribution. Thus we have the function describing the PE spectrum

$$S(E, T) = \int_{-\infty}^{+\infty} d\epsilon \left[ \frac{dN(\epsilon, T)}{d\epsilon} + C \right] g(E - \epsilon) f(\epsilon, T), \quad (4)$$

with the spectrometer function  $g(E)$  and the Fermi-Dirac distribution  $f(E, T) = [\exp(E/k_B T) + 1]^{-1}$ . Note that the Fermi-Dirac distribution has an independent, absolute temperature scale which cannot be expressed by the reduced temperature  $T/T_c$ . For the description of the transfer of spectral weight by thermal excitations we define the absolute temperature by setting  $T_c = T_c(\text{V}_3\text{Si}) = 17.1$  K in this Fig. 1.

For the numerical simulation of the data, the BCS DOS can be integrated analytically over the finite step size  $\delta E$  of the spectra, avoiding problems with the divergence at  $\pm \varepsilon(T)$ . The discrete convolution with the spectrometer function was performed via a fast-Fourier transform [16].

Figure 2 shows the experimental data above (filled circles,  $T = 19$  K) and below the transition temperature (open circles,  $T = 11$  K). The normal metallic spectrum above  $T_c$  can be described by a constant DOS (normalized to unity), which is cut off by the Fermi-Dirac distribution of the respective temperature and convoluted with the spectrometer resolution function. Lowering the sample temperature significantly below  $T_c$  has two dramatic effects on the PE spectra: A narrow peak appears at an energy of  $E = -3.9$  meV, and the spectral weight at  $E_F$  drops by more than a factor of 5. In addition, a small peak

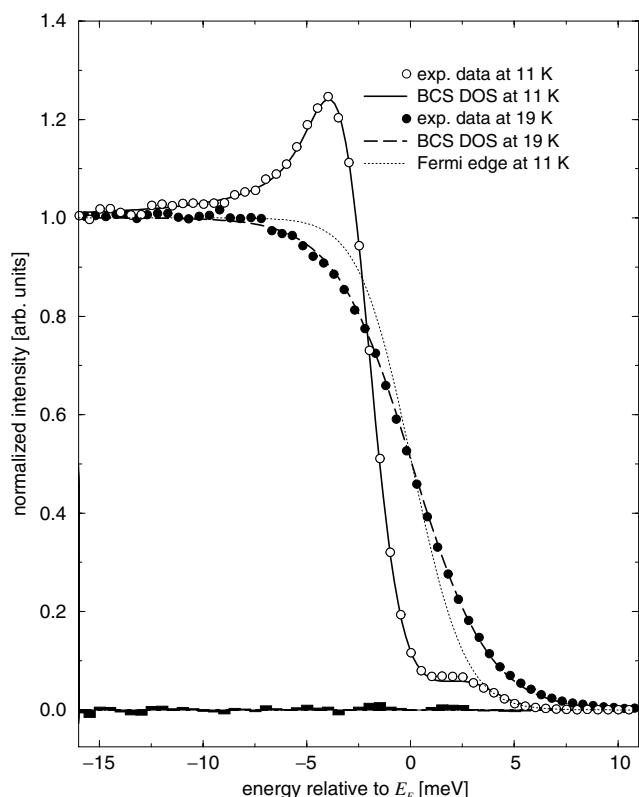


FIG. 2. Comparison of experimental data at  $T = 11$  and  $19$  K with the broadened BCS density of states. Free parameters of the least-squares fit: energy resolution  $\Delta E = 2.9$  meV, gap width  $\varepsilon(11 \text{ K}) = 2.5$  meV, normal conducting fraction of the surface  $C/(1 + C) = 13\%$ . The dotted line describes a metallic Fermi edge at  $T = 11$  K. The residuum of the fit at  $11$  K is given as black bars at the bottom of the figure.

appears at  $E \approx 2$  meV above  $E_F$  which is the residue of the thermally occupied singularity of the BCS DOS. Taking into account the finite energy resolution, this is exactly what would anticipate from the BCS theory (cf. Fig. 1).

The solid and the dashed line in Fig. 2 display the numerically modeled spectra at  $T = 11$  K and  $T = 19$  K, respectively, given by Eq. (4). The other parameters of the theoretical spectrum are  $\Delta E = 2.9$  meV and a (half) gap width of  $\varepsilon(11 \text{ K}) = 2.5$  meV, which is close to the zero temperature value  $\varepsilon_0$ . Published values of  $\varepsilon_0$  of  $\text{V}_3\text{Si}$  are in the range of  $\varepsilon_0 = 2.6 \pm 0.2$  meV [4,5,7,8]. Although the photoemission information depth is limited to approximately  $10\text{--}20 \text{ \AA}$  at this photon energy, the analysis of the spectra of various samples gives good agreement with the results from bulk sensitive measurements: If there are particular surface properties, the consequence for the transition temperature  $T_c$  is small. On the other hand, we assume that normal metallic contributions at the surface lead to the high intensity in the gap region, which we describe by a fraction of  $C/(1 + C) = 13\%$  to the total spectrum  $S(E, T)$ . A different data modeling with a distribution of different transition temperatures (instead of the normal conducting fraction) could not explain the high intensity in the gap and the shape of the spectra near  $E_F$ .

The importance of the energy resolution is demonstrated in Fig. 3. The solid line represents the modeled spectrum

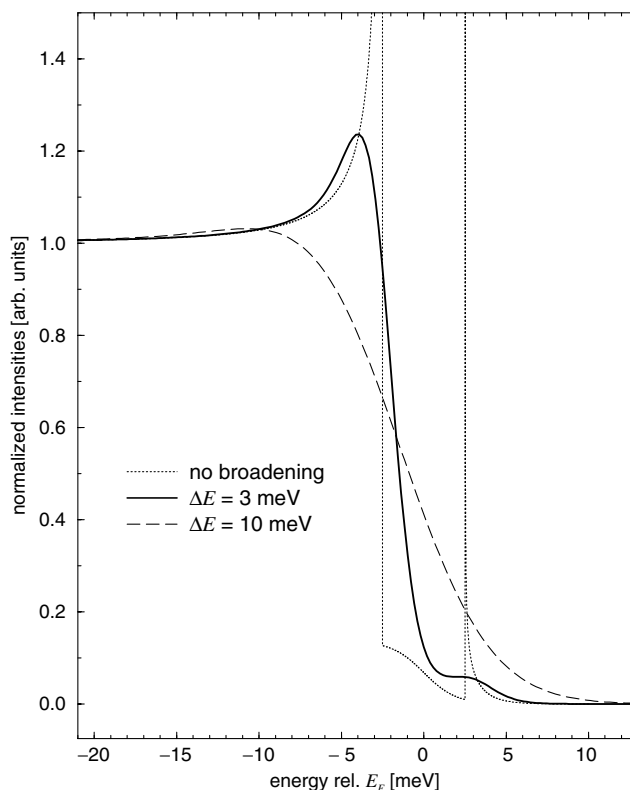


FIG. 3. Importance of energy resolution to the photoemission spectra. Modeled spectrum for  $T = 11$  K from Fig. 2 (solid line) in comparison to unbroadered DOS (dotted) and spectrum with increased energy resolution of  $\Delta E = 10$  meV (dashed).

for the 11 K data. Removing the experimental broadening yields the mere BCS DOS with a total gap width of  $\Delta_{\text{gap}} = 2\epsilon(T) = 5.0$  meV plus the normal conducting contribution, visible inside the gap (dotted line). Already at an energy resolution of  $\Delta E = 10$  meV (dashed) there is nearly no resemblance to the BCS line shape left. A careful comparison to the broadened Fermi-Dirac distribution at this temperature would show the opening of the gap as a small energy shift of the edge of about 1–2 meV to lower energies.

Figure 4 shows the energy range close to the Fermi level of another  $V_3\text{Si}$  sample for three different temperatures  $T = 12, 15,$  and  $20$  K. The gap decreases from  $\epsilon(12 \text{ K}) = 2.3$  meV to  $1.2$  meV at  $T = 15$  K, and disappears completely for the spectrum at  $T = 20$  K. The dotted line is equivalent to the modeled spectrum at 12 K but without the normal conducting contribution ( $C = 0$ ), which was set to 15% for the other calculated curves. The consequence of the finite value of  $C$  is (a) the filling of the gap range, that has—due to the energy broadening with a FWHM of about 3 meV—its minimum at 0.8 meV above  $E_F$ , and (b) the decreasing peak intensity of the BCS peak below  $E_F$ . The solid lines give the respective

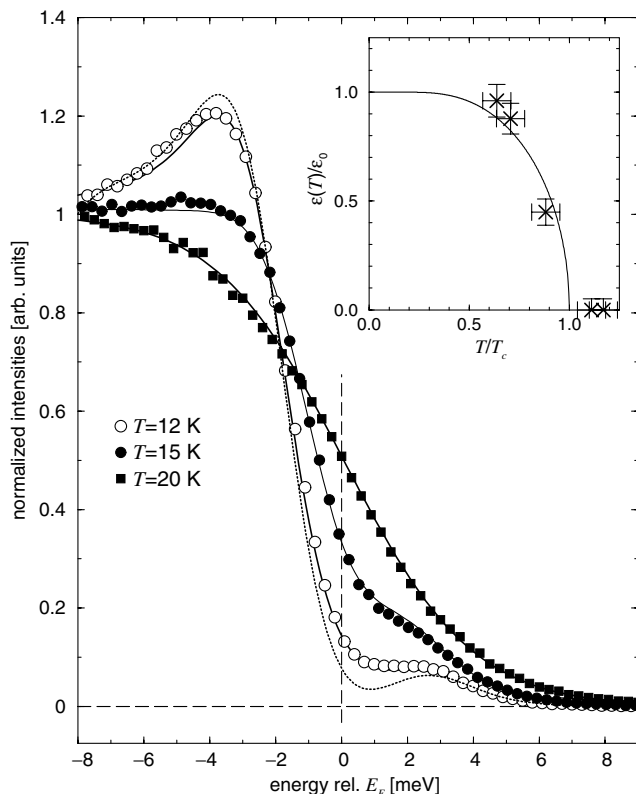


FIG. 4. Gap range of  $V_3\text{Si}$  for three different temperatures. The solid lines give the respective fits with the parameters  $\Delta E = 2.8$  meV,  $C/(1 + C) = 15\%$ ,  $\epsilon(T) = 2.3$  meV (12 K),  $1.2$  meV (15 K), and  $0$  meV (20 K). The dotted line gives the modeled spectrum at  $T = 12$  K without normal metallic contribution ( $C = 0$ ), all other parameters unchanged. The inset shows gap size vs reduced temperature  $T/T_c$  (as extracted from the least-squares fit).

model curves, with only one changed parameter  $T$ , i.e., the sample temperature during the measurement given in the figure captions). The inset in Fig. 4 summarizes the results of the analysis of the data in Figs. 2 and 4 in the form of the reduced gap width  $\epsilon(T)/\epsilon_0$  in the form of the reduced gap width  $\epsilon(T)/\epsilon_0$  versus the reduced temperature  $T/T_c$ , following the predictions for a weak-coupling limit superconductor within the experimental errors (solid line).

In conclusion, we have measured for the first time the photoemission spectra of a conventional superconducting A15 alloy, in which both the phase transition at  $T_c$  and the BCS characteristics—superconducting gap and the enhancement of the DOS at either  $\pm\epsilon(T)$ —are clearly observable. Furthermore, the analysis of the spectra, based on simple BCS theory, gives quantitative results which are in accordance with the data published in the literature. In particular, these quantitative results do not point to a significant influence of surface effects to the superconducting properties of the surface sampled by PES. Our experiments form the basis for extended measurements of gap anisotropies and Fermi surface topologies on single crystalline samples by use of high-resolution photoemission spectroscopy in the meV scale.

We would like to thank Dr. Paul Steiner (Saarbrücken) for stimulating discussions. This work was supported by the Deutsche Forschungsgemeinschaft (HU 149/19-1 and SFB 277).

\*Corresponding author.

Email: friedel@mx.uni-saarland.de

- [1] J. G. Bednorz and K. A. Müller, *Z. Phys. B* **64**, 189 (1986).
- [2] J. Bardeen, L. N. Cooper, and J. R. Schrieffer, *Phys. Rev.* **108**, 1175 (1957).
- [3] J. Müller, *Rep. Prog. Phys.* **43**, 641 (1980).
- [4] S. B. Dierker, M. V. Klein, G. W. Webb, and Z. Fisk, *Phys. Rev. Lett.* **50**, 853 (1983).
- [5] R. Hackl, R. Kaiser, and S. Schickantz, *J. Phys. Condens. Matter* **16**, 1792 (1983).
- [6] R. Hackl, R. Kaiser, and W. Gläser, *Physica (Amsterdam)* **162C–164C**, 431 (1989).
- [7] T. J. B. Janssen, C. Haworth, S. M. Hayden, P. Meeson, M. Springford, and A. Wasserman, *Phys. Rev. B* **57**, 11 698 (1998).
- [8] J. Schumann, *Phys. Status Solidi B* **99**, 79 (1980).
- [9] J. Kwo and T. H. Geballe, *Phys. Rev. B* **23**, 3230 (1981).
- [10] K. E. Kihlstrom, *Phys. Rev. B* **32**, 2891 (1985).
- [11] Z. Shen and D. S. Dessau, *Phys. Rep.* **253**, 1 (1995).
- [12] M. Gioni, D. Malterre, B. Dardel, J.-M. Imer, Y. Baer, J. Müller, J. L. Jorda, and Y. Petroff, *Phys. Rev. B* **43**, 1216 (1991).
- [13] A. R. Sweedler and D. E. Cox, *Phys. Rev. B* **12**, 147 (1975).
- [14] G. Nicolay, F. Reinert, S. Schmidt, D. Ehm, P. Steiner, and S. Hüfner, *Phys. Rev. B* **62**, 1631 (2000).
- [15] T. Jarlborg, A. A. Manuel, and M. Peter, *Phys. Rev. B* **27**, 4210 (1983).
- [16] W. H. Press, B. P. Flannery, S. A. Teukolsky, and W. T. Vetterling, *Numerical Recipes in C—The Art of Scientific Computing* (Cambridge University Press, Cambridge, 1990).